Bastian Zehner[1,*]

Wolfgang Korth[1]

Fabian Schmidt[2]

Mirza Cokoja[2]

Andreas Jess[1]

Kinetics of Epoxidation of Cyclooctene with Ionic Liquids Containing Tungstate as Micellar Catalyst

The kinetics of cyclooctene epoxidation with H_2O_2 by micellar catalysis was studied. As catalyst, an ionic liquid (IL) containing the catalytically active tungstate anion was used. The tungstate IL forms micelles in the aqueous H_2O_2 phase. It is simply formed by dissolving sodium tungstate and 1-octyl-3-methylimidazolium tetrafluoroborate [OMIM][BF_4] in aqueous H_2O_2. For the epoxidation of cyclooctene by micellar catalysis, a power law kinetic model was determined that takes the critical micelle concentration into account. The kinetics of the [OMIM][BF_4]/Na_2WO_4 catalyst is similar to pure [OMIM]$_2$[WO_4], which indicates that the active species is formed in situ. Addition of phenylphosphonic acid improves the activity of the tungstate IL. The most effective catalyst was tested in a semi-continuous and continuous loop reactor.

1 Introduction

Epoxides are important intermediates for the industrial production of consumer bulk chemicals such as ethylene glycol or polyethylene glycols (PEGs). The most important epoxides are ethylene oxide and propylene oxide. As only ethylene oxide can be produced economically by direct epoxidation with molecular oxygen from ethylene, propylene oxide is synthesized industrially via heterogeneous catalysis using zeolites like titanium silicalite-1 (TS-1) [1]. However, also longer-chain epoxides are needed for fine chemicals. As common substrates long-chain olefins are used [2]. State-of-the-art for the industrial production of long-chain epoxides are processes using the Prilezhaev reaction. In this reaction, the olefin is oxidized by percarboxylic acids, which are formed in situ from the corresponding carboxylic acid and aqueous H_2O_2. The low solubility of the long-chain olefins in the aqueous phase requires the addition of chlorinated or aromatic solvents to the biphasic system to achieve high reaction rates. The use of these chemicals is contended because they are considered hazardous to the environment and health. Hence, alternative processes for the epoxidation of longer-chain olefins are desirable.

The low solubility of the oxidant in the organic phase can be circumvented by phase transfer catalysis [3]. The best-known examples are the catalyst systems developed by Noyori and Venturello [4, 5]. Phase transfer catalysis relies on a catalyst that shuttles between the biphasic system, in many cases an aqueous phase and an organic phase. The catalyst activates the reactant in the aqueous phase and transports it to the reactant in the organic phase where the reaction takes place. In this case, an organic solvent is required to guarantee sufficient solubility for the phase transfer catalyst and the organic reactant.

As water is considered a green solvent, another approach is to increase the solubility of the organic reactant in the aqueous phase. This can be achieved by adding surface-active substances, which are capable of forming micelles in water. These micelles act as nanoreactors [6, 7]. The benefits of micellar catalysis are that the effective epoxidation catalyst shows high solubility in water and has low affinity to leach into the organic phase and is easily prepared. After the reaction, the product moves in the organic phase and can be separated. Certain ionic liquids (Ils) form micelles in water and therefore are the surfactants needed.

ILs are highly promising candidates for micellar catalysis as they are versatile and have unique properties that can be fine-tuned to the system of interest [8, 9]. ILs having long-chain alkyl groups form micelles in water and can be modified on a molecular basis to fit the needs of the reaction under investigation (solubility, catalytic active anion, etc.) [10–12].

In a previous paper, an approach to determine the kinetics of a 1-octyl-3-methylimidazolium perrhenate [OMIM][ReO_4]-catalyzed micellar catalysis was presented [13, 14]. Therein, the micellar catalyst system was prepared by simply dissolving the

---

[1]Bastian Zehner, Dr. Wolfgang Korth, Prof. Dr.-Ing. Andreas Jess
bastian.zehner@uni-bayreuth.de
Chair of Chemical Engineering, Faculty of Engineering Science, Universitaetsstrasse 30, 95447 Bayreuth, Germany.

[2]Fabian Schmidt, Dr. Mirza Cokoja
Chair of Inorganic and Metal-Organic Chemistry, Faculty of Chemistry and Catalysis Research Center, Technical University of Munich, Ernst-Otto-Fischer-Strasse 1, 85747 Garching bei München, Germany.

IL [OMMIM][BF$_4$] and NaReO$_4$ in aqueous H$_2$O$_2$, although both compounds separately are catalytically inactive in olefin epoxidation. By this procedure, the active [OMIM][ReO$_4$] catalyst evolves and forms micelles facilitated by the tetrafluoroborate ionic liquid. This method avoids the laborious synthesis of pure [OMIM][ReO$_4$].

As the tungstate anion is known as active species in the catalysis of epoxidation reactions, a tungstate IL micellar catalyst was prepared using the same protocol [15, 16]. This micellar catalyst showed improved activity. For the system 1-octyl-3-methylimidazolium tetrafluoroborate [OMMIM][BF$_4$] and tungstate [WO$_4$]$^{2-}$ the most active system with regard of cyclooctene (COE) epoxidation was screened, the kinetics were investigated, and the most active catalyst was tested in a continuous loop reactor.

2 Experimental

2.1 Materials

The IL catalyst [OMIM]$_2$[WO$_4$] was synthesized according to a protocol as previously reported [17]. The ILs for in situ preparation of the catalyst [OMIM][BF$_4$] and [OMIM] were purchased from IoLiTec-Ionic Liquids Technologies GmbH, Germany. Na$_2$WO$_4$, H$_2$WO$_4$, COE (> 95 %), and phenylphosphonic acid were obtained from AlfaAesar. Aqueous H$_2$O$_2$ (H$_2$O$_2$ > 49 wt %, as confirmed with permanganate titration) used in the experiments was delivered by VWR chemicals and produced in France. All chemicals named above were taken as received without further purification.

2.2 Experimental Setup and Catalytic Experiments

All catalytic experiments were conducted at ambient pressure and at temperatures ranging from 30 to 70 °C. Batch experiments were carried out in a 10-mL cylindrical glass reactor with a septum for probe extraction and a reflux condenser cooled with water. The reactor was heated in an oil bath and the reaction mixture stirred with a magnetic stirrer. If not mentioned otherwise, the batch experiments were conducted with 2.8 mL (20 mmol) COE as organic phase; the molar composition of the 2.9 mL aqueous phase was 50 mmol H$_2$O$_2$ (and consequently 96 mmol H$_2$O), 1 mmol of [OMIM][BF$_4$], and 0.5 mmol of the catalytic active tungstate salt. The temperature was 70 °C and the stirring rate 1200 rpm. Before the COE was introduced, the aqueous phase was preheated to reaction temperature. The stirrer speed was set to 1200 rpm. To take samples, the stirring was stopped and the phases allowed to separate. Samples were dissolved in 1 mL heptane in a 1.5-mL glass vial. For the variation of the H$_2$O$_2$ or COE concentration, the components were substituted by H$_2$O and cyclooctane, respectively.

For the continuous operation, a water-heated stainless-steel reactor equipped with static mixers (supplied by Fluitec) was used. A circular pump recirculated the aqueous phase within the reactor. The aqueous phase formed after leaving the reactor was recirculated back via a peristaltic pump. The COE was charged via an HPLC pump (Knauer 5-mL pump head). Before the experiments 250 g of aqueous phase was produced (molar ratio 50:1:0.5:1 H$_2$O$_2$/[OMIM]$^+$/[WO4]$^{2-}$/PPA; PPA denotes phenylphosphonic acid) and transferred into the reactor and feed tank for the aqueous phase. After reaching the reaction temperature, the organic reactant was charged into the reactor using the HPLC pump. Thereby, the reaction was started. Because of the high volumetric flow rate of the aqueous phase the loop reactor can be regarded as a continuous stirred-tank reactor (CSTR) reactor.

2.3 Evaluation of the Experiments

The conversion of COE was determined via analysis of the organic phase as only small amounts of reactant and product are present in the aqueous phase [18]. The samples were taken from the organic phase while the stirring was stopped. Because the amount of organic material solubilized in the aqueous phase is very low, it can be assumed that the composition in the organic phase represents the composition in the whole system. The samples were analyzed by a Bruker 450 gas chromatograph (GC) equipped with an Ultra 2 column (50 m, 0.32 mm, 0.5 µm) and a flame ionization detector (FID). The reaction is highly selective and only cyclooctene oxide (COO) and no byproducts could be detected. Hence, the conversion X[1]) was determined according to the following equation:

$$X = \frac{n_{COO}}{n_{COE} + n_{COO}} \tag{1}$$

In Eq. (1), the conversion of COE is calculated using the areas of the individual compounds as detected by GC. The reaction rate was calculated for the consumption of COE according to Eq. (2). For the reaction is biphasic, the reaction rate is expressed with regard to the volume of the aqueous phase, i.e., the phase where the reaction takes place:

$$r = -\frac{1}{V_{aq}} \frac{dn_{COE}}{dt} \tag{2}$$

3 Results and Discussion

3.1 Mass Transport Limitations in the Batch Experiments

For the intrinsic kinetic parameters, the influence of mass transport has to be excluded. In our epoxidation system, the transfer of the olefin from the organic into the aqueous catalyst phase may be strongly influenced by mass transport limitations. An experimental series was conducted with varying stirring rates of the magnetic stirring bar (molar ratio 50:1:0.5:1 H$_2$O$_2$/[OMIM]$^+$/Na$_2$WO$_4$/PPA; 50 °C). The stirring rate ranged from 400 to 1600 rpm in steps of 200 rpm. With increasing

---

1) List of symbols at the end of the paper.

stirring rate, the organic droplets in the emulsion were reduced in size, which led to a higher surface area between both phases. The data showed that the reaction rate increased at higher stirring rates and no homogeneous mixture was formed for stirring rates below 1000 rpm. At 1200 rpm the reaction mixture changed to a white emulsion and the reaction rate reached a maximum. Further increase of the stirring rate left the reaction rate unchanged. The higher stirring rate has no effect on the form or size of the micelles. Hence, mass transport limitations could be excluded.

3.2 Solubility of the Reactant in the Aqueous Phase

In a biphasic reaction it is essential to know the concentration of the reactants in the phase where the reaction actually happens over time to get the kinetic parameters. Moreover, it is of interest to have information on the amount of the other organic compounds, i.e., product and organic solvent. In the biphasic reaction system described herein, the reaction occurs in the aqueous phase, and thus, the amount of organics and the composition of the organics in the catalyst phase are needed to gain information on the concentration of the reactant that is available for the epoxidation (see simplified scheme in Fig. 1).
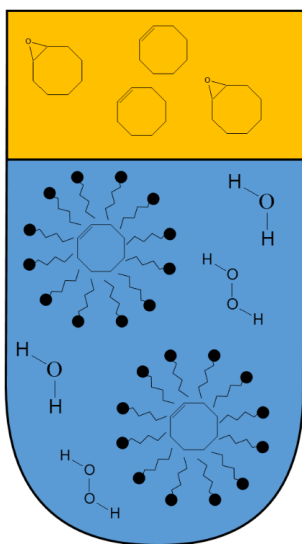

Figure 1. Simplified scheme of cyclooctene epoxidation with the micelle-forming tungstate ILs in the aqueous phase with 50 wt % H_2O_2. During the reaction the solution is stirred.

In the case of micellar catalysis, this corresponds to the amount of olefin embedded in the micelles present in the aqueous phase, at any given time of reaction. In addition, it is necessary to know if the micelles contain every component of the reaction in equal parts in solution, i.e., olefin and H_2O_2. For the solubility of the organic phase the solubility coefficient was calculated by Eq. (3):

$$K_{solv} = \frac{n_{COE}}{n_{IL}} = \frac{n_{COE,micelles} + n_{COE,H2O2}}{n_{IL} - n_{cmc,IL}(T)} \qquad (3)$$

The so-called critical micelle concentration (cmc_{IL}) is the minimal IL concentration, at which micelles are formed. As the solubility of COE in aqueous H_2O_2 is very low, the term $c_{COE,H2O2}$ can be neglected and Eq. (3) reduces to Eq. (4):

$$K_{solv} = \frac{n_{COE,micelles}}{n_{IL} - n_{cmc,IL}(T)} \qquad (4)$$

The concentration of COE in the aqueous phase during epoxidation was determined by GC. Before GC analysis the COE was extracted from the aqueous phase with heptane. Cyclohexene served as standard. For K_{solv}, a value of 0.12 was obtained for OMIMBF$_4$ at 70 °C. As illustrated in Fig. 2, the olefin concentration in the micelles (that is in the aqueous phase) remains constant with changing composition of the organic phase until COO made up a molar fraction of 0.7 in the organic phase. This indicates that the micelles selectively take up the olefin and release the epoxide into the organic phase. At epoxide concentrations above a molar fraction of 0.7, the solubility of [OMIM][BF$_4$] and therefore the tungstate catalyst associated with it increases in the organic phase, which lowers the ability of the IL to dissolve the olefin (here COE) in the aqueous phase.
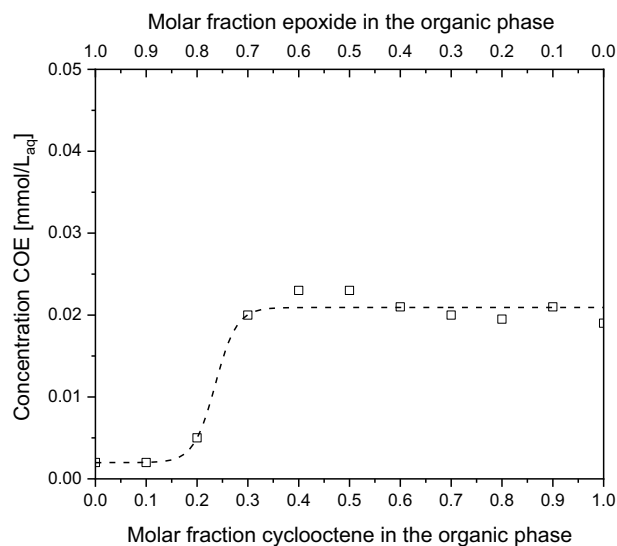

Figure 2. Solubility of cyclooctene in 17 mol L^{-1} hydrogen peroxide at 70 °C with 350 mmol L^{-1} [OMIM]BF$_4$ at various degrees of molar fractions of the corresponding epoxide cyclooctenoxide. The dashed line indicates the trend.

3.3 Screening of the Tungstate Catalyst for Micellar Epoxidation

In our previous work [14], we have reported that sodium tungstate with [OMIM]Cl is a promising catalytic system for the epoxidation of COE using aqueous H_2O_2 in a biphasic micellar setup. The screening was focused on the structure-reactivity relationship of the alkyl chain length at the imidazolium cation and the IL counteranion. First, the surface-active ILs [OMIM]X (X = Cl$^-$, [BF$_4$]$^-$) of the previous work were catalytically tested

with soluble tungstate salts (Na_2WO_4, K_2WO_4) and tungstic acid H_2WO_4. Experiments were conducted at 70 °C in a Schlenk-like glass vessel with a volume of 10 cm^3. Then the stirring speed was set to 1200 rpm eliminating mass transfer limitations. The experiments were evaluated concerning reaction rate and H_2O_2 stability. The concentration of the IL was 350 mmol L^{-1} and of the tungstate salt 175 mmol L^{-1}, respectively.

The data of selected batch experiments of the screening are presented in Fig. 3. The micellar catalytic systems of [OMIM]Cl or [OMIM][BF_4] with Na_2WO_4 showed initially similar reaction rates as the more acidic catalytic system with tungstate acid, but a rapid decomposition of H_2O_2 in the aqueous phase is observed. In the experiments H_2O_2 was present in a great excess, but only 27 % and 44 % of the COE was converted to the epoxide, because the residual H_2O_2 was completely decomposed to oxygen and water. Replacing Na_2WO_4 by H_2WO_4 resulted in the case of [OMIM]Cl in a similar initial rate with a higher stability of the H_2O_2 and thus a higher conversion of COE of up to 80 %. In the case of [OMIM][BF_4]/H_2WO_4 complete conversion was quickly obtained with little decomposition of H_2O_2, but the selectivity to the epoxide was considerably lower (< 70 %) in comparison to the other catalyst/IL systems. A 1:1 mixture of the sodium salt and tungstatic acid yielded good reaction rates, low decomposition of H_2O_2, a selectivity of over 99 %, and complete conversion of COE after about 300 min. This in agreement with our previous results that chloride inhibits the epoxidation [14].
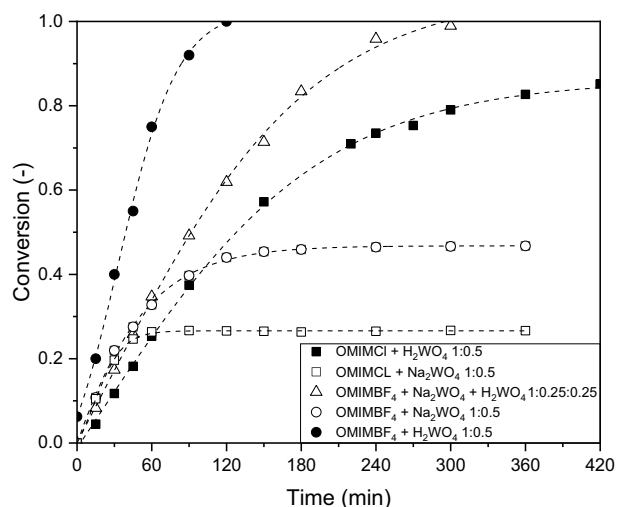

Figure 3. Screening for the best mixture of [OMIM][BF_4] and [OMIM]Cl and tungstate salts in batch experiments. Concentration of IL 350 mmol L^{-1}, tungstate salt 175 mmol L^{-1}, respectively; T = 70 °C, H_2O_2 concentration 17 mol L^{-1}, stirring rate 1200 min^{-1}.

As seen in Fig. 3, the presence of Cl^- ions leads to a lower reaction rate (comparison of [OMIM]Cl and [OMIM][BF_4] with H_2WO_4). These results were confirmed by adding NaCl to the more active systems; the sodium chloride inhibited the reaction rate (Fig. 4). This can be explained by the lower pH value of the aqueous solution with the tungstate acid catalyst. It is known that the pH value is highly important for the stability
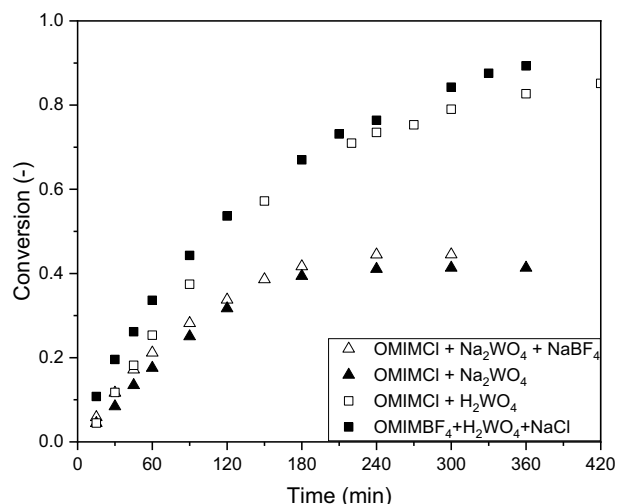

Figure 4. Influence of different anions on the reaction rate of the epoxidation of cyclooctene. Concentration of IL 350 mmol L^{-1}, tungstate salt 175 mmol L^{-1}, respectively; T = 70 °C, H_2O_2 concentration 17 mol L^{-1}, stirring rate 1200 min^{-1}.

of epoxides. If the pH value is too low, acid-catalyzed ring opening can occur resulting in diol formation. It was also observed that adding NaCl to the [OMIM][BF_4]/H_2WO_4 system resulted in similar reaction rates and stability of H_2O_2 than the [OMIM]Cl/H_2WO_4 system (Fig. 4). The best micellar catalyst/IL system is a mixture of Na_2WO_4 and H_2WO_4 in equimolar fractions and [OMIM][BF_4] as IL.

3.4 Kinetics of Cyclooctene Epoxidation

For the kinetic model a simple power law equation was used. Because the concentration of the tungstate catalyst was held constant at 350 mmol L^{-1} in all kinetic experiments, it was united with the "true" kinetic constant k' to an overall rate constant k:

$$r_{COE} = k' c_{WO_4^{2-}} c_{H2O2}^a c_{COE,aq}^b = k c_{H2O2}^a c_{COE,aq}^b \qquad (5)$$

The reaction order of H_2O_2 was determined by a variation of the concentration of H_2O_2 (dilution of the 50 wt % H_2O_2 with demineralized water). The volume of the aquatic phase was thereby kept constant. The catalyst concentration was 175 mmol L^{-1} (corresponding to 0.175 mmol L^{-1} Na_2WO_4/H_2WO_4 and 350 mmol L^{-1} [OMIM][BF_4]). Fig. 5 depicts that the reaction is of first order with regard to H_2O_2, which is in contrast to a second order in the perrhenate-catalyzed epoxidation. Obviously, the reaction pathways are different. Perrhenate activates H_2O_2 via an outer-sphere mechanism, i.e., activation of H_2O_2 without influence of metal atom in the center. For this mechanism two H_2O_2 molecules are needed, explaining the second order. The first order for H_2O_2 in case of tungstate indicates an inner sphere mechanism.

To determine the reaction order of COE, a gradual substitution of COE by cyclooctane (COA) was conducted. COA is very similar in structure and size, and thus, it can be assumed
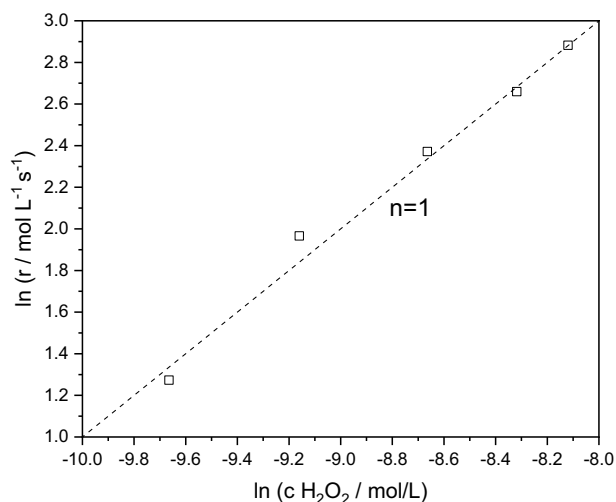
Figure 5. Determination of the reaction order of hydrogen peroxide through variation of the H_2O_2 concentration in the aqueous phase, the slope determines the order. Concentration of IL 350 mmol L^{-1}, tungstate salt 175 mmol L^{-1}, respectively; $T = 70\,°C$, H_2O_2 concentration 17 mol L^{-1}.

that both are identically embedded in the micelles. The volume of the organic phase was held constant. The experiments were conducted at 70 °C, the concentration of the in situ formed active IL $[OMIM]_2[WO_4]$ was 175 mmol L^{-1}. Fig. 6 illustrates that the epoxidation reaction is of first order with regard to COE. However, the conversion curve obtained in the screening experiments indicates that the (apparent) reaction order is rather zero, at least up to 70 % conversion of COE (constant slope of conversion versus time, see Fig. 3).

Furthermore, the influence of the product concentration was investigated. COO in the organic phase has no influence on the
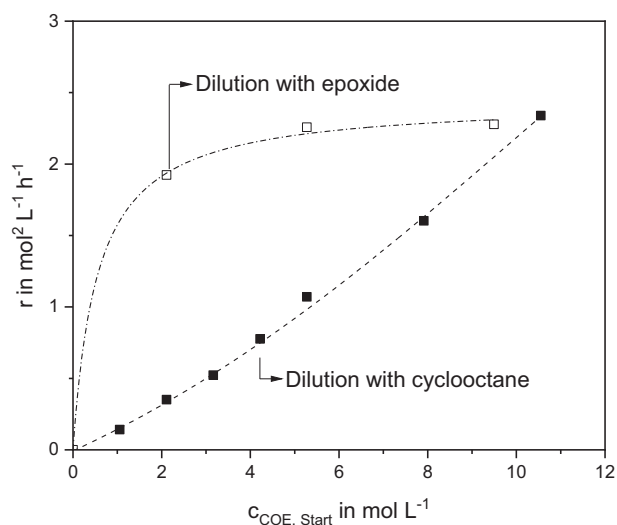

Figure 6. Influence of the dilution of the organic phase with cyclooctane or epoxide on the reaction rate of the epoxidation; Concentration of IL 350 mmol L^{-1}, tungstate salt 175 mmol L^{-1}, respectively; $T = 70\,°C$, H_2O_2 concentration 17 mol L^{-1}, stirring rate 1200 min^{-1}.

rate until the concentration of the reactant in the organic phase gets below the maximum uptake of organic reactant of the micelles (Fig. 6). After this point the rate drops due to the declining concentration of reactant in the aqueous phase. This confirms the results shown in Fig. 2: the olefin is preferably solved by the micelles, which leads to a constant COE content in the aqueous phase and a constant composition of the organic phase solubilized by the micelles until the fraction of COE in the organic phase gets very low (< 0.3). Due to the not changing organic composition solubilized in the aqueous phase, the reaction rate does not change until a high conversion of more than about 70 % is reached (Fig. 3, $[OMIM][BF_4]$ with Na_2WO_4/ H_2WO_4) despite of the lower concentration of COE in the whole system. This leads to an apparent zero-order reaction even though the measurements with COA addition confirm that the reaction is intrinsically first order with regard to COE.

The activation energy was determined by temperature variation in the range of 30–90 °C. The experiments were conducted with a similar catalyst composition as during H_2O_2 concentration variation. However, the IL concentration had to be corrected with the *cmc* value. A part of the IL is not participating in micelle formation; this concentration is called critical micelle concentration, *cmc*. As displayed in Fig. 7, at IL concentrations below the *cmc* no micelles are formed and the reaction rate is very low due to the low solubility of COE. Above the *cmc*, micelles are formed and the solubility and in turn also the reaction rate increase strongly and linearly.
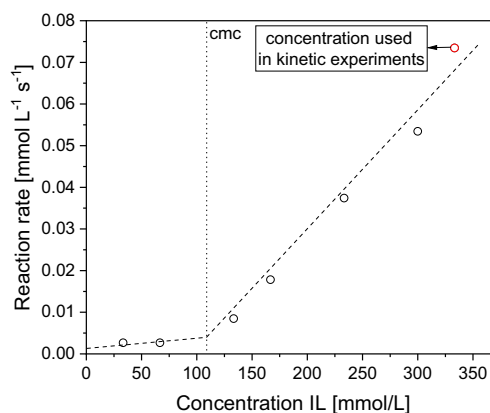

Figure 7. Reaction rate versus IL concentration. Below the critical micelle concentration (here about 110 mmol L^{-1}) the rate is very low due to the low solubility of COE in the aqueous phase (no micelles). Above the *cmc*, the solubility increases with rising IL concentration. Concentration of OMIMBF$_4$ 0–350 mmol L^{-1}, tungstate salt 175 mmol L^{-1}, respectively; $T = 70\,°C$, H_2O_2 concentration 17 mol L^{-1}, stirring rate 1200 min^{-1}.

The *cmc* is dependent on the surfactant, solvent, and temperature as already measured in our previous work [19]. Because the amount of IL before micelles are formed does not participate in the reaction and the *cmc* is a temperature-dependent value, the concentration of the IL was adapted in the temperature variation.

$$c_{IL,cat}(T) = c_{IL} - cmc_{IL}(T) \tag{6}$$

The activation energy and the pre-exponential factor were calculated by the Arrhenius equation:

$$\ln k = \ln k_0 - \frac{Ea}{RT} \qquad (7)$$

The activation energy is $49\,\text{kJ mol}^{-1}$ ($k_o = 8000\,\text{L mol}^{-1}\text{s}^{-1}$), which is in agreement with literature data [1, 20, 21].

The kinetic data were applied to a Matlab model for a batch reactor. It was thereby assumed that the concentration of COE in the aqueous phase is constant (see Fig. 2) until less COE is present in the organic phase than needed to fill the micelles in the aqueous phase. So, in the initial phase of epoxidation, typically until a conversion of about 70 % is reached, the concentration of the remaining COE in the organic phase is given by Eq. (8):

$$c_{\text{COE,aq}}(T) = K_{\text{solv}}(c_{\text{IL}} - cmc(T)) \qquad (8)$$

If there is less COE in the organic phase than needed for the micelles, the concentration is given by:

$$c_{\text{COE,aq}} = \frac{n_{\text{COE,organic phase}}}{V_{\text{aq}}} \qquad (9)$$

The change of concentration of H_2O_2 was calculated based on the assumption that H_2O_2 is only consumed by epoxidation and not by decomposition, which is negligible in the glass reactors. Fig. 8 demonstrates that the model describes the experiments very well.

3.5 Improving the Reaction Rate of Epoxidation by Addition of Phenylphosphonic Acid

Noyori et al. [4] reported that the addition of phenylphosphonic acid (PPA) accelerates the rate of epoxidation in phase transfer catalysis without affecting the selectivity of the reac-

tion. Thus, PPA was added to the micellar catalytic system. With the mixture of the tungstate salts Na_2WO_4 and H_2WO_4 for the in situ formation of the catalytic active IL, the reaction rate was strongly improved, but on the expense of epoxide selectivity because of the low pH value of the aqueous phase due to PPA. To prevent the selectivity loss, the catalyst salt was changed from a mixture of Na_2WO_4/H_2WO_4 to only Na_2WO_4. The best molar ratio of PPA to tungstate anion determined in the screening experiments was 2:1; a further increase of the PPA concentration showed no effect on the reaction rate.

Fortunately, PPA did not influence the stability of H_2O_2 and a selectivity of H_2O_2 towards the epoxidation was determined to 93 %. Further experiments led to the conclusion that PPA neither does not act as phase transfer agent nor does it change the solubility of the organic reactant in the aqueous phase. CryoTEM pictures confirmed that the micellar structure was not altered by this additive [17]. Surface tension measurements also approved that PPA had no influence on the *cmc*. Moreover, the proposed [OMIM]BF_4 + Na_2WO_4/PPA catalytic system showed the same kinetics as the pure [OMIM]$_2WO_4$ IL with PPA.

For this new catalytic system, the parameters of the power law kinetics needed to be re-evaluated. The reaction orders of COE and H_2O_2 did not change. This indicates a mechanism similar to the micellar catalyst without PPA, but the reactive tungstate species changes, as we reported previously [17]. However, the activation energy was lower ($42\,\text{kJ mol}^{-1}$), resulting in a considerably higher rate constant, i.e., $0.006\,\text{L mol}^{-1}\text{s}^{-1}$ at 40 °C compared to only $0.000045\,\text{L mol}^{-1}\text{s}^{-1}$ without PPA addition.

3.6 Applying Micellar Catalysis for Cyclooctene Epoxidation in a Continuous Reactor

With regard to a technical application, the developed catalyst was tested in a continuous setup with a loop reactor. Due to the high circulation rate and the slow separation of the two
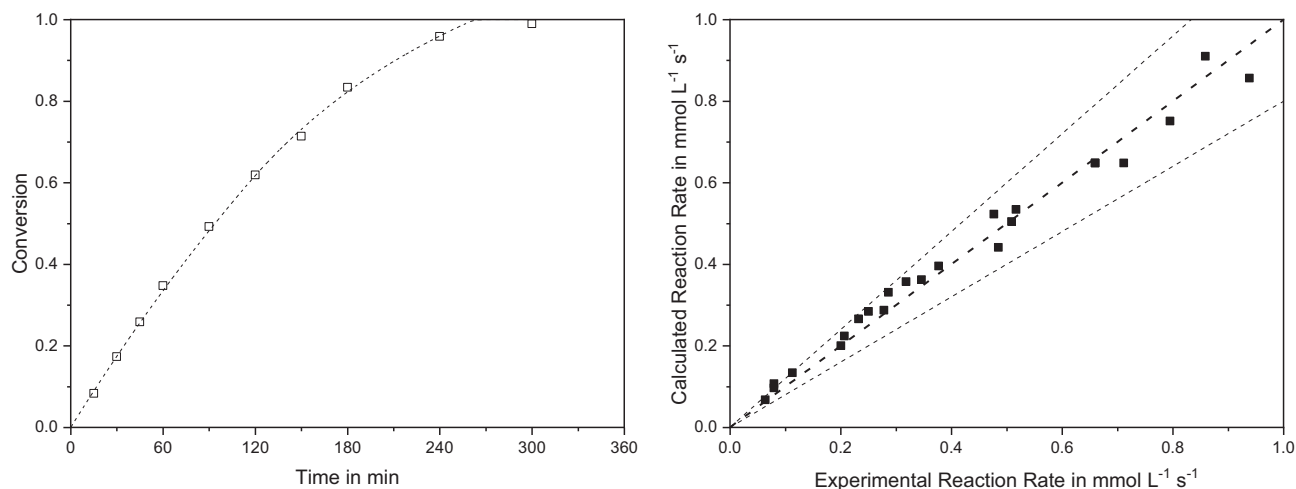

Figure 8. Comparison of the experimental data (squares) with the model (dotted line). Conversion over reaction time in a batch experiment. Temperature 70 °C; H_2O_2 concentration 17 mol L^{-1}; concentration [OMIM][BF$_4$] 350 mmol L^{-1}; concentration $Na_2WO_4+H_2WO_4$ (1:1) 175 mmol L^{-1} (left); parity plot of the data used for the determination of the kinetics (right).

phases, an external separator was used. The loop reactor can be regarded as a CSTR, which was confirmed by the measurement of the residence time distribution, being very close to an ideal CSTR. The H_2O_2 in the solution demanded an inert reactor material in terms of decomposition of H_2O_2, and the reactor also had to be resistant to corrosion caused by H_2O_2. The best materials in terms of these demands, costs, and applicability are glass and stainless steel (1.4404). The reactor and the static mixers were made of stainless steel, the separator was made of glass.

For circulation, a rotary pump was used with a corrosion-free pump head. Here, an HPLC pump was chosen for dosing the organic phase; for the aqueous phase, a hose pump was used. As micellar agent and catalyst for the continuous experiments the IL $[OMIM]_2[WO_4]$ with the additive phenylphosphonic acid (molar ratio 1:2) was taken, as this is the most active micellar catalyst with regard to epoxidation and a low activity towards H_2O_2 decomposition. However, prior to the epoxidation experiments, it was again tested that the H_2O_2 in the aqueous phase did not decompose significantly in the reactor at reaction conditions (max. 60 °C). The concentration of H_2O_2 in the aqueous phase only decreased by 10 % in 120 min, which can be regarded as acceptable. For comparison with the continuous epoxidation experiments, a Matlab model of the CSTR was developed and the kinetic data given in Sect. 3.5 were used.

Fig. 9 presents the experimental and simulated data of the continuous epoxidation of COE with the CSTR setup. At 60 °C, a conversion of more than 80 % was reached, which was constant over 2 h. The slight decline in conversion is due to the decreasing H_2O_2 concentration in the aqueous phase upon consumption by decomposition and epoxidation. The feed rate of the aqueous phase was 10 mL min^{-1} to replenish the H_2O_2 in the reactor. The organic phase feed rate was 1 mL min^{-1}. The selectivity of H_2O_2 to epoxidation was 92 %, the residual H_2O_2 decomposed due to te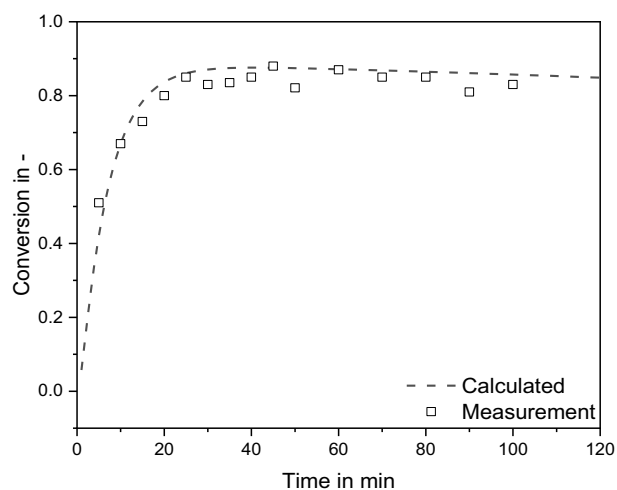mperature and contact with the reactor surface. The selectivity to the epoxide turned out to be greater than 99 %. The kinetic model of the CSTR describes the experimental data very accurately.

4   Conclusion

The epoxidation of COE was conducted with tungstate in micellar catalysis. It was demonstrated that the IL $[OMIM]_2[WO_4]$ shows similar reaction rates and selectivity as the mixture of $[OMIM][BF_4]$ and Na_2WO_4. The $[OMIM][BF_4]$ tungstate system could be strongly improved by using a mixture of H_2WO_4 and Na_2WO_4 as catalyst. The addition of PPA to the aqueous phase improved the reaction rate considerably without a negative effect on selectivity and stability of H_2O_2. The kinetics of the epoxidation was determined with and without the additive. The kinetic data suggest that the reaction mechanism is altered by the additive by changing the active species. The kinetic data was used to model a CSTR for the continuous epoxidation of COE with good agreement with the experiments.

Acknowledgment

Symbols used

c_i	[mol L^{-1}]	concentration of compound i
cmc	[–]	critical micelle concentration
k	[L mol^{-1}s^{-1}]	reaction rate constant with catalyst concentration
k'	[L^{2}mol^{-2}s^{-1}]	reaction rate constant
k_0	[L mol^{-1}s^{-1}]	pre-exponential factor
K_{Solv}	[–]	solubility constant
n_i	[mol]	molar amount of compound i
r	[mol L^{-1}s^{-1}]	reaction rate
t	[h]	time
T	[K]	temperature
V	[L]	volume
X	[–]	conversion

Subscripts

aq	aqueous phase
IL	ionic liquid

Abbreviations

COA	cyclooctane
COE	cyclooctene
COO	cyclooctane oxide
CSTR	continuous stirred-tank reactor
HPLC	high-performance liquid chromatography

Figure 9. Conversion rate in a continuous experiment at 60 °C with the $[OMIM]_2WO_4$ catalyst and the additive PPA. Concentration of $OMIM_2WO_4$ 175 mmol L^{-1}, PPA 350 mmol L^{-1}, H_2O_2 17 mol L^{-1}, volume flow of reactant 1 mL min^{-1}, volume flow of aqueous phase 10 mL min^{-1}. Recirculation rate 1200 min^{-1}.

IL   ionic liquid
OMIM   1-methyl-3-octyl imidazolium
PPA   phenylphosphonic acid

References

[1] S. Kwon, N. M. Schweitzer, S. Park, P. C. Stair, R. Q. Snurr, *J. Catal.* **2015**, *326*, 107–115. DOI: https://doi.org/10.1016/j.jcat.2015.04.005

[2] *Ullmann's Encyclopedia of Industrial Chemistry*, Wiley-VCH, Weinheim **2000**.

[3] M. Mąkosza, M. Fedoryński, *Catal. Rev.* **2003**, *45 (3–4)*, 321–367. DOI: https://doi.org/10.1081/CR-120025537

[4] R. Noyori, M. Aoki, K. Sato, *Chem. Commun.* **2003**, *16*, 1977–1986. DOI: https://doi.org/10.1039/b303160h

[5] C. Venturello, E. Alneri, M. Ricci, *J. Org. Chem.* **1983**, *48 (21)*, 3831–3833. DOI: https://doi.org/10.1021/jo00169a052

[6] S. R. Yetra, T. Rogge, S. Warratz, J. Struwe, W. Peng, P. Vana, L. Ackermann, *Angew. Chem., Int. Ed.* **2019**, *58 (22)*, 7490–7494. DOI: https://doi.org/10.1002/anie.201901856

[7] K. Bica, P. Gartner, P. J. Gritsch, A. K. Ressmann, C. Schroder, R. Zirbs, *Chem. Commun.* **2012**, *48 (41)*, 5013–5015. DOI: https://doi.org/10.1039/c2cc31503c

[8] *Ionic Liquids in Organometallic Catalysis* (Eds: J. Dupont, L. Kollár), Topics in Organometallic Chemistry, Springer, Berlin **2015**.

[9] S. Werner, M. Haumann, P. Wasserscheid, *Annu. Rev. Chem. Biomol. Eng.* **2010**, *1*, 203–230. DOI: https://doi.org/10.1146/annurev-chembioeng-073009-100915

[10] M. Blesic, M. H. Marques, N. V. Plechkova, K. R. Seddon, L. P. N. Rebelo, A. Lopes, *Green Chem.* **2007**, *9 (5)*, 481. DOI: https://doi.org/10.1039/b615406a

[11] F. Geng, J. Liu, L. Zheng, L. Yu, Z. Li, G. Li, C. Tung, *J. Chem. Eng. Data* **2010**, *55 (1)*, 147–151. DOI: https://doi.org/10.1021/je900290w

[12] C. Jungnickel, J. Łuczak, J. Ranke, J. F. Fernández, A. Müller, J. Thöming, *Colloids Surf., A* **2008**, *316 (1–3)*, 278–284. DOI: https://doi.org/10.1016/j.colsurfa.2007.09.020

[13] J. Schäffer, B. Zehner, W. Korth, M. Cokoja, A. Jess, *Chem. Eng. Technol.* **2019**, *42 (1)*, 232–240. DOI: https://doi.org/10.1002/ceat.201800399

[14] J. Schäffer, M. Alber, W. Korth, M. Cokoja, A. Jess, *ChemistrySelect* **2017**, *2 (35)*, 11891–11898. DOI: https://doi.org/10.1002/slct.201702709

[15] G. B. Payne, P. H. Williams, *J. Org. Chem.* **1959**, *24 (1)*, 54–55. DOI: https://doi.org/10.1021/jo01083a017

[16] K. Yamaguchi, C. Yoshida, S. Uchida, N. Mizuno, *J. Am. Chem. Soc.* **2005**, *127 (2)*, 530–531. DOI: https://doi.org/10.1021/ja043688e

[17] F. Schmidt, B. Zehner, W. Korth, A. Jess, M. Cokoja, *Catal. Sci. Technol.* **2020**, *10 (13)*, 4448–4457. DOI: https://doi.org/10.1039/D0CY00673D

[18] M. Cokoja, R. M. Reich, M. E. Wilhelm, M. Kaposi, J. Schäffer, D. S. Morris, C. J. Münchmeyer, M. H. Anthofer, I. I. E. Markovits, F. E. Kühn, W. A. Herrmann, A. Jess, J. B. Love, *ChemSusChem* **2016**, *9 (14)*, 1773–1776. DOI: https://doi.org/10.1002/cssc.201600373

[19] B. Zehner, F. Schmidt, W. Korth, M. Cokoja, A. Jess, *Langmuir* **2019**, *35 (49)*, 16297–16303. DOI: https://doi.org/10.1021/acs.langmuir.9b02759

[20] W. Feng, Y. Wang, G. Wu, Y. Lin, J. Xu, H. Shi, T. Zhang, S. Wang, X. Wu, P. Yao, *J. Chem. Technol. Biotechnol.* **2015**, *90 (8)*, 1489–1496. DOI: https://doi.org/10.1002/jctb.4462

[21] N. J. Schoenfeldt, Z. Ni, A. W. Korinda, R. J. Meyer, J. M. Notestein, *J. Am. Chem. Soc.* **2011**, *133 (46)*, 18684–18695. DOI: https://doi.org/10.1021/ja204761e